

Low energy fast events from radon progenies at the surface of a CsI(T ℓ) scintillator

S.C. Kim,^{a,1} H. Bhang,^a J.H. Choi,^a W.G. Kang,^b H.J. Kim,^c
K.W. Kim,^a S.K. Kim,^{a,2} Y.D. Kim,^b H.S. Lee,^a J.I. Lee,^a
J.H. Lee,^a J.K. Lee,^a M.J. Lee,^a S.J. Lee,^a J. Li,^a J. Li,^d
Y.J. Li,^d X. Li,^a S.S. Myung,^a S.L. Olsen,^a S. Ryu,^a
I.S. Seong,^a J.H. So,^c Q. Yue^d
(KIMS Collaboration)

^a*Department of Physics and Astronomy, Seoul National University, Seoul 151-742, Korea*

^b*Department of Physics, Sejong University, Seoul 143-747, Korea*

^c*Physics Department, Kyungpook National University, Daegu 702-701, Korea*

^d*Department of Engineering Physics, Tsinghua University, Beijing 100084, China*

Abstract

In searches for rare phenomena such as elastic scattering of dark matter particles or neutrinoless double beta decay, alpha decays of ^{222}Rn progenies attached to the surfaces of the detection material have been identified as a serious source of background. In measurements with CsI(T ℓ) scintillator crystals, we demonstrate that alpha decays of surface contaminants produce fast signals with a characteristic mean-time distribution that is distinct from those of neutron- and gamma-induced events.

Key words: alpha, ^{222}Rn , CsI(T ℓ) crystal, dark matter, pulse shape discrimination

1 Introduction

Signals caused by radioactive decays of ^{222}Rn progenies that adhere to detector surfaces are known to be serious background for rare phenomena experiments such as searches for WIMPs (Weakly Interacting Massive Particles)

¹ sckim@hep1.snu.ac.kr

² skkim@hep1.snu.ac.kr

dark matter and neutrinoless double beta decay [1,2,3]. ^{222}Rn is a noble gas that permeates the air. It decays to ^{218}Po , which is a reactive metal that readily adheres to almost any surface [4]. Through successive decay chains, the progenies of ^{222}Rn can accumulate on detector surfaces. When they decay, only a portion of the energy of the decay products is detected, thereby producing a troublesome low energy background. Among the progenies of ^{222}Rn , ^{210}Pb and ^{210}Po are the most dangerous because they have long half-lives, 22.3 years and 138 days, respectively. If an experimental system is isolated, ^{210}Po becomes the principal alpha emitting contaminant. The energy spectrum of these surface events appears as a continuum that ranges from the full peak energy of the alpha down to the very low energies. Anomalously fast events have been observed in WIMP search experiments that use inorganic scintillators, and these have been attributed to the effects of surface alpha (SA) events since their rate is seen to be reduced when the detector surfaces are polished [1,5,6]. The KIMS experiment at the Yangyang Underground Laboratory in Korea looks for WIMP-induced nuclear recoils in an array of CsI(Tl) scintillators [7]. Figure 1 shows a scatter plot of energy deposits versus LMT10 for events seen in the KIMS detector, where LMT10 denotes the natural logarithm of the mean-time of each event calculated for a 10 μs interval starting from the beginning of the event ($\text{LMT10} = \frac{\sum_{t_i < 10\mu\text{s}} A_i \times t_i}{\sum_{t_i < 10\mu\text{s}} A_i}$, A_i is the area of the i^{th} cluster, which is usually equivalent to a single photo-electron, of an event). In the lower right-hand portion of the plot, strong alpha-decay peaks can be seen with tails that extend down to zero energy and low LMT10 values. Here one can see that LMT10 values for the low energy tail events are distinctly smaller than those from gamma-ray induced signals.

WIMPs are expected to scatter elastically from nuclei. The KIMS experiment is designed to detect the energy deposited by the recoiling nucleus and uses a pulse shape discrimination (PSD) analysis to distinguish nuclear recoil events from gamma-induced backgrounds [7]. The presence of surface alpha events at energies below 10 keV, the main region of interest for the dark matter search, complicates the PSD analysis.

2 Experimental setup

In order to investigate the characteristics of SA background events, we contaminated the surface of a small CsI(Tl) sample crystal with ^{222}Rn progenies by placing it for four days in a special chamber at the Korea Research Institute of Standards and Science (KRISS) in which the ^{222}Rn concentration was around 4.33 MBq/m³. The size of the contaminated crystal is 3 cm \times 3 cm \times 1.4 cm.

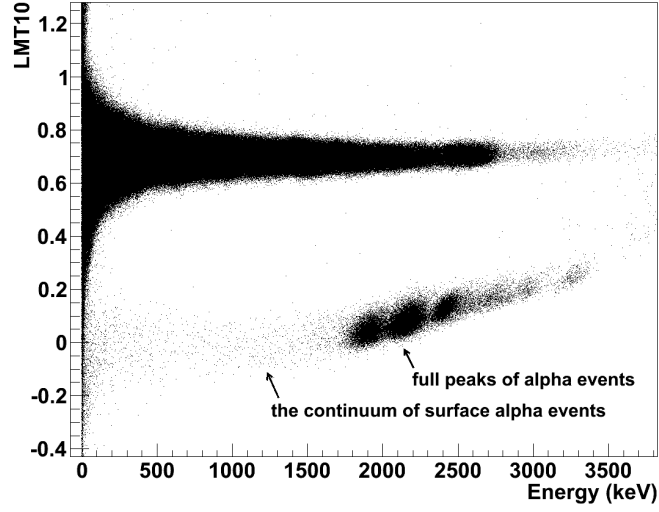


Fig. 1. Deposited energy (horizontal) versus LMT10 (vertical) in data from the KIMS experiment. Here LMT10 denotes the natural logarithm of the mean-time of each event computed over first 10 μs interval. Here one can see that SA events are present as a band whose LMT10 is small compared to the background, which indicates that they decay quickly.

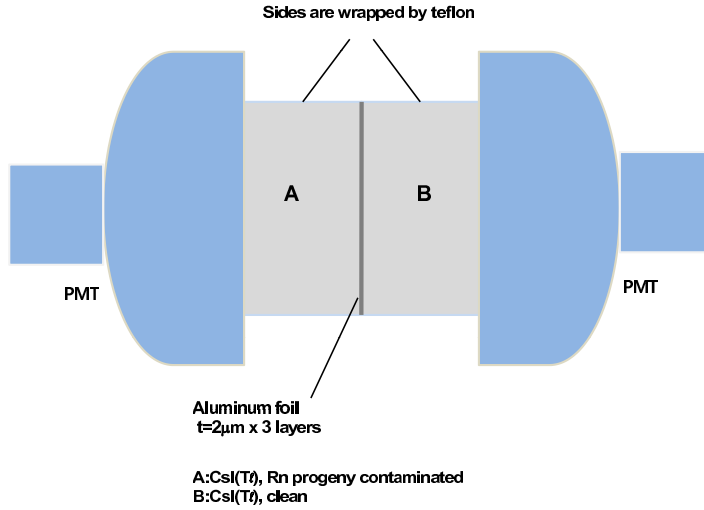


Fig. 2. A schematic depiction of the Radon progenies contaminated Double crystal Detector (RDD). Crystal A is the ^{222}Rn -progenies contaminated CsI(Tl) crystal and crystal B is a clean CsI(Tl) crystal that is used to detect an alpha particle that escapes from crystal A. The two crystals are separated by three 2 μm -thick layers of aluminum foil.

The parent ^{222}Rn nucleus decays to ^{218}Po with a half-life of 3.8 days. In a period of several tens of minutes, the ^{218}Po nucleus decays to ^{210}Pb via several decay steps. ^{210}Pb beta decays with a half-life of 22.3 years to ^{210}Bi , which subsequently beta decays to ^{210}Po . From this series of beta decays, ^{210}Po , the main source of surface alpha events, is continuously produced on the crystal surface. It decays into ^{206}Pb with a half-life of 138 days, emitting a 5304 keV alpha particle. The kinetic energy of the recoiling ^{206}Pb nucleus is 103 keV.

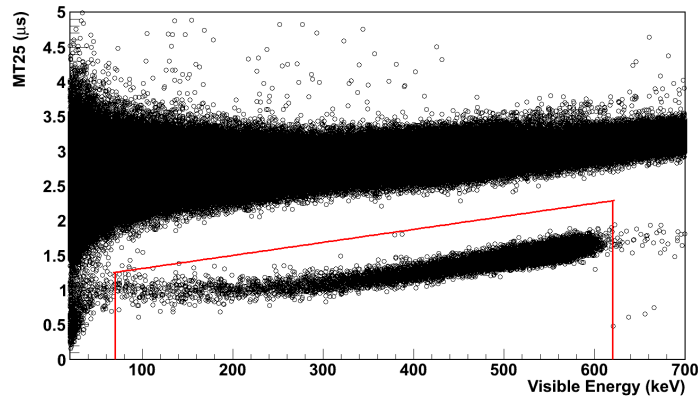


Fig. 3. MT25 versus the visible energy in crystal B, where MT25 is the mean-time of each event that is determined over a 25 μs event-time window. The events inside the red solid lines are selected as alphas escaping from crystal A.

Figure 2 shows a schematic diagram of the experimental setup, which we named the Radon progenies contaminated Double crystal Detector (RDD), that was used to study the characteristics of SA events. In order to tag escaping surface alpha particles, we attached a clean CsI(Tl) crystal (crystal B in Fig. 2) to a face of the contaminated one (crystal A in Fig. 2). We inserted three 2 μm -thick aluminum foils between the two crystals to provide a barrier to prevent cross-talk of the scintillation light between the crystals that the 5 MeV alphas can easily penetrate. According to the SRIM program [8], the energy loss of a 5304 keV alpha in a 6 μm -thick aluminum layer is 998 keV; thus alphas that penetrate the foils still have ample energy to provide a trigger signal. These layers also serve as a reflector for the collection of scintillation light. The sides of the crystals are wrapped with teflon tape. A 3 inch photomultiplier tube (PMT), 9269QA from Electron Tubes, Ltd. is attached to each crystal to detect the scintillation photons. The PMT signals are amplified 100 times by a fast amplifier from Notice Co., Ltd. The amplified signals are digitized by a 400 MHz Flash Analog-to-Digital Converter (FADC) of Notice Co., Ltd. that is mounted in a Versa Module Eurocard (VME) crate that is read-out by a linux-operating PC via a VME-USB2 interface. The DAQ system is based on the ROOT package [9]. When two or more photoelectrons (PEs) are detected in each PMT within a 2 μs time window, a trigger is generated. Events with pulse width longer than 300 ns are also triggered in order to include high energy events in which many PEs are merged into a single big pulse. For each

event, the PMT responses throughout a $40.96 \mu\text{s}$ time window is recorded. Of these, pulses inside a $25 \mu\text{s}$ window are used for analysis.

To tag SA events in crystal A, we require a signal in crystal B that is consistent with that of an alpha particle. Because of the good PSD power of CsI(Tl) scintillators, as shown in Fig. 3, alpha signals are clearly separated from other backgrounds. Here, MT25, the mean-time of each event determined over a $25 \mu\text{s}$ time window, is used. In Fig. 3, the visible energy is the measured energy which differs from the actual energy above around 100 keV because of the saturation effect resulting from the DAQ system optimized for collecting low energy events. Furthermore, the energy of alpha events is underestimated more by the quenching factor in CsI(Tl), which is about 0.5. No corrections for these effects have been applied. Events that populate the region inside the red solid lines of Fig. 3 are selected as alphas that escape from crystal A. Figure 4 shows a scatter plot of energy in crystal A versus the visible energy in crystal B for events tagged as alphas. This figure shows the sum of the energies at both crystals has an upper bound, as expected. The wide spread in the sum of the energies reflects the energy loss in the Al foil layers and possible dead layer on the surface of the detector, which depends upon the alpha particle's direction. To separate SA events from background, an upper bound of alpha energy at crystal B is set at 620 keV and a lower bound at 70 keV. The experiment started two months after the radon contamination of the crystal was done and ran for about 3 months. The rate of events tagged as SA increased with time because of the continuous supply of ^{210}Po from ^{210}Pb . The event rate became 947 events/day by the end of the measurement period. From this value, the amount of ^{210}Pb contaminants implanted at the surface of the crystal is estimated to be about 1.6×10^8 and the adhesion rate of radon progenies in the radon chamber is estimated to be about $13/\text{cm}^2/\text{s}$.

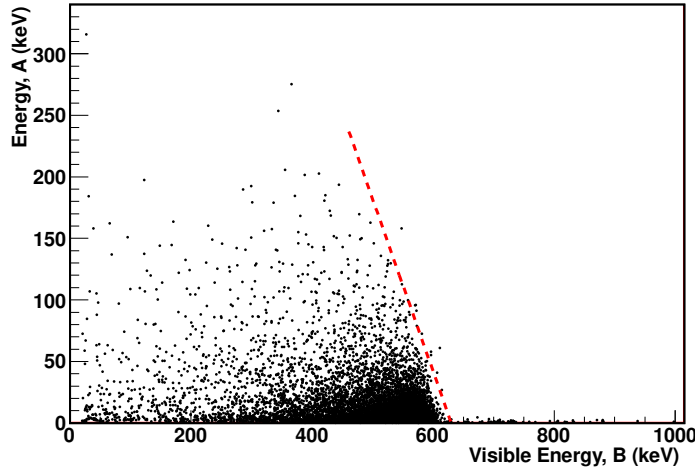


Fig. 4. Energy of crystal A versus the visible energy of crystal B for events that are tagged as an alpha.

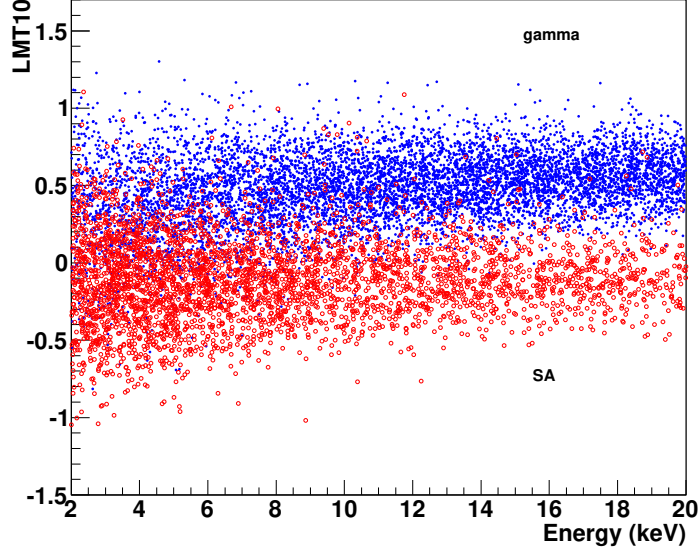


Fig. 5. LMT10 of SA events and gamma events in RDD

3 Mean-time distribution of SA events

In the KIMS experiment, the quantity LMT10 is used as the PSD discriminator. The distribution of LMT10 for SA events must be understood in order to distinguish them from dark matter candidate events in KIMS. For this we analyzed the response of crystal A in the SA-tagged events selected according to the description in the previous section.

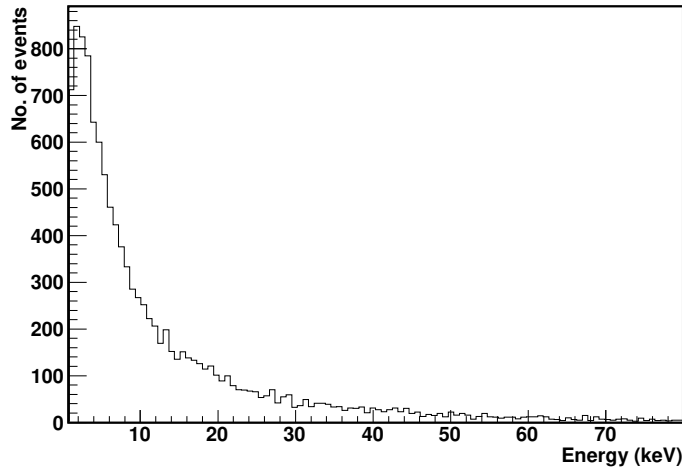


Fig. 6. The energy spectrum in crystal A for SA-tagged events.

Figure 5 shows the LMT10 distribution for SA- and gamma ray-induced events from RDD in the low energy range that is used in the dark matter search. The

SA events range down to 3 keV, the energy threshold for this study. Figure 6 shows the energy spectrum of SA events. The energy deposited in crystal A is the sum of the recoil energy of the recoiling ^{206}Pb nucleus and some partial energy of the alpha particle. The ^{206}Pb recoil energy is 103 keV, and it is expected to show up as 7–8 keV due to the quenching factor of CsI(Tl) if we assume the quenching factor for ^{206}Pb is the same as that for Cs and I nuclei [10,11]. The FWHM energy resolution at this energy is 4 keV. There is no clear ^{206}Pb signal such as that which was seen in another study that used a phonon sensor [3]. The scintillator may have an inactive surface layer where the scintillation efficiency is very small that it can cause smearing of ^{206}Pb signal.

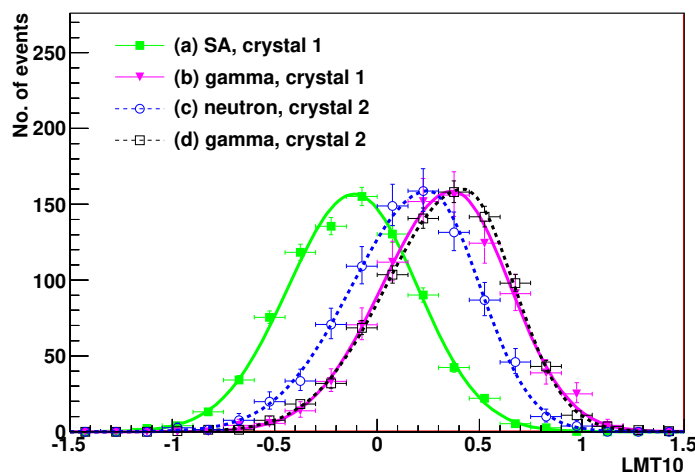


Fig. 7. LMT10 distributions for various reference data at 3 keV. (a) LMT10 for SA-induced events in crystal 1, (b) gamma-induced events in crystal 1, (c) neutron-induced events in crystal 2 and (d) gamma-induced events in crystal 2.

The LMT10 distributions for 3–4 keV energy bin are shown in Fig. 7. The crystal used for the SA study with ^{222}Rn contamination is labeled crystal 1 in the figure; the crystal used for the neutron response study is a different crystal, crystal 2, which was exposed to an Am-Be neutron source. Here, we also present the results of gamma calibration for both test crystals for comparison. The gamma calibration was done by irradiating the crystals with ^{137}Cs source. The temperature for SA study setup was maintained as $(25.4 \pm 0.3)^\circ\text{C}$, and for neutron study setup, $(25.3 \pm 0.7)^\circ\text{C}$. The results in the figure show that SA-induced signals are, on average, faster than neutron-induced signal events, and their LMT10 distributions are distinct. Figure 8 shows the value of the peak position of LMT10 distribution as a function of the energy for each type of event, which is not necessarily same with the mean value since the distribution is an asymmetric Gaussian. The SA LMT10 distribution obtained from this study is used to distinguish possible WIMP-induced nuclear recoils from surface alpha-induced events in the KIMS data.

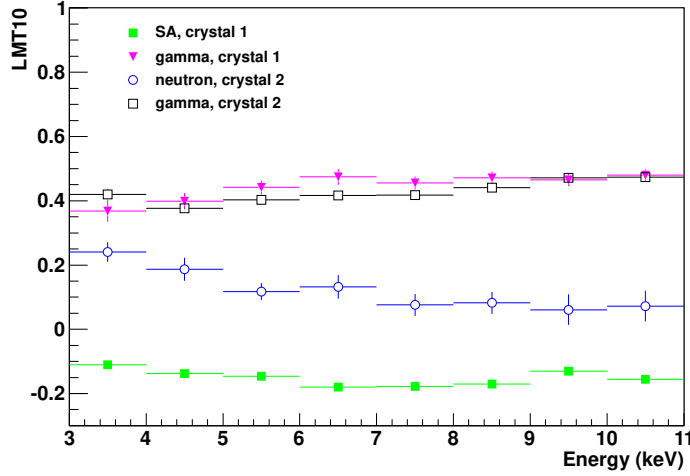


Fig. 8. The value of the peak position of LMT10 distributions for SA-, neutron- and gamma-induced events. Crystal 1 refers to the crystal used for SA study and crystal 2 is the one used for the neutron response measurement.

4 Conclusion

We have studied surface alpha background from ^{222}Rn progenies with a CsI(Tl) scintillator contaminated with ^{222}Rn progenies, mainly ^{210}Pb and its daughters. The main alpha emitter is ^{210}Po . When ^{210}Po alpha decays at the surface, it doesn't deposit its full energy into the detector. Its energy spectrum ranges from the full peak energy to the very low energy. We directly show that SA events decay faster than neutron and gamma events. We also obtained the distribution of LMT10, the PSD parameter, for SA events. This can be used to analyse the dark matter search data of KIMS experiment.

Acknowledgments

We thank Dr. Jongman Lee for providing us access to the KRISS radon chamber. We are very grateful to the Korea Midland Power Co. and their staff for providing the underground laboratory space at Yangyang. This research was supported by the WCU program (R32-10155) and Basic Science Research Program (2010-0005332) through National Research Foundation of Korea funded by the Ministry of Education, Science and Technology.

References

- [1] V. A. Kudryavtsev *et al.*, *Astropart. Phys.* **17**, 401 (2002).
- [2] M. Pavan *et al.*, *Eur. Phys. J. A* **36**, 159 (2008).
- [3] R. F. Lang *et al.*, *Astropart. Phys.* **33**, 60 (2010).
- [4] S. Cooper *et al.*, *Phys. Lett. B* **490**, 6 (2000).
- [5] V. A. Kudryavtsev *et al.*, *Phys. Lett. B* **452**, 167 (1999).
- [6] N. J. T. Smith *et al.*, *Phys. Lett. B* **485**, 9 (2000).
- [7] H. S. Lee *et al.*, *Phys. Rev. Lett.* **99**, 091301 (2007).
- [8] J. F. Ziegler, J. P. Biersack and U. Littmark, *The Stopping and Range of Ions in Matter*, SRIM Co., Chester, Maryland (2008).
- [9] R. Brun and F. Rademakers, ROOT - An Object Oriented Data Analysis Framework, Proceedings of AIHENP '96 Workshop, Lausanne, Sep. 1996; *Nucl. Instrum. Methods A* **389**, 81 (1997), see also <http://root.cern.ch>.
- [10] H. Park *et al.*, *Nucl. Instrum. Methods A* **491**, 460 (2002).
- [11] V. I. Tretyak, *Astropart. Phys.* **33**, 40 (2010).